Lithium ion sites and their contribution to the ionic conductivity of RLi$_2$O-B$_2$O$_3$ glasses with $R \leq 1.85$

Anne Ruckman [a], Graham Beckler [a], William Guthrie [a], Martha Jesuit [a], Makyla Boyd [a], Ian Slagle [a], Robert Wilson [a], Nathan Barrow [b], Nagia S. Tagiara [c], Efstratios I. Kamitsos [c], Steve Feller [a], Caio B. Bragatto [a,*]

[a] *Physics Department, Coe College, Physics Department, Cedar Rapids, IA 52402, USA*
[b] *Johnson Matthey Technology Centre, Blount's Court, Sonning Common, Reading RG4 9NH, UK*
[c] *Theoretical and Physical Chemistry Institute, National Hellenic Research Foundation, 48 Vassileos Constantinou Ave., 11635 Athens, Greece*

ARTICLE INFO

ABSTRACT

The ionic conductivity in lithium borate glasses RLi$_2$O-B$_2$O$_3$ is believed to be related to the number of loose lithium ions, calculated using the topological constraint theory, increasing significantly when $0 \leq R \leq 0.5$ and reaching a plateau when $0.5 \leq R \leq 1.0$, and increasing once again when $R \geq 1.0$. To test this new proposed approach, high content lithium oxide glasses were prepared (up to $R = 1.85$) without any signs of heterogeneity by using a fast quenching technique. Results show that instead of being related to the number of loose lithium ions, the ionic conductivity is mostly likely related to the different boron species which act as lithium sites, given that the number of non-bridging oxygens increases proportionally to the lithium to boron ratio when $R \geq 0.5$, the region where the plateau in electrical properties is observed.

1. Introduction

Ionically conductive glasses have been studied for a long time, but there are still many open questions about the fundamental mechanisms behind this phenomenon [8]. The interest goes beyond the fundamental understanding, with these glasses being applied as solid state ionics for batteries [22] and sensors [24]. Since ionic conductivity is related to the movement of ions when an electric field is applied to the glass, an interest resides in understanding how these mobile ions are bound to the structure and interact with it, affecting the activation energy of the process.

A peculiar case can be found for lithium borate glasses (RLi$_2$O-B$_2$O$_3$). Both the activation energy and the absolute values for ionic conductivity appear to reach a plateau value when $R \geq 0.5$. This behavior has been observed up to $R = 1.0$; above this composition the glasses become harder to prepare without crystallization, although a few cases can be found in the literature [1,6,11,12,28,33].

Verhoef [32] justified the existence of two species of Li$^+$ according to the coordination number of B, given by the equation:

$$Li^{Loose} = R - Li^{NB} \tag{1}$$

where Li^{Loose} and Li^{NB} are the number of lithium ions associated with four-coordinated borons (N$_4$) and the number of lithium ions associated with each non-bridging oxygen (NBO) per boron, respectively. Li^{Loose} and Li^{NB} were found experimentally by Kamitsos [17] and observed using molecular dynamics by Varsamis [29] and Vegiri [31].

In the literature, it is common to find the glass composition as xLi$_2$O-(1-x)B$_2$O$_3$. For clarity, the relationship between x and R is given by the equation:

$$R = \frac{x}{1-x} \tag{2}$$

Takeda and collaborators applied a topological constraint model to the system, predicting, with accuracy, some of the glass properties, such as the glass transition temperature (T$_g$) [27]. In this work, the authors propose the existence of two different Li$^+$ species, classifying them according to their bond rigidity with the glass matrix; loose or clustered Li$^+$.

When compared to experimental values for ionic conductivity in the literature, the relationship between the number of loose lithium ions and the ionic conductivity shows a similar behavior up to $R = 1$, but above this value Takeda's model predicts another increase in conductivity,

---

* Corresponding author.
E-mail address: cbragatto@coe.edu (C.B. Bragatto).

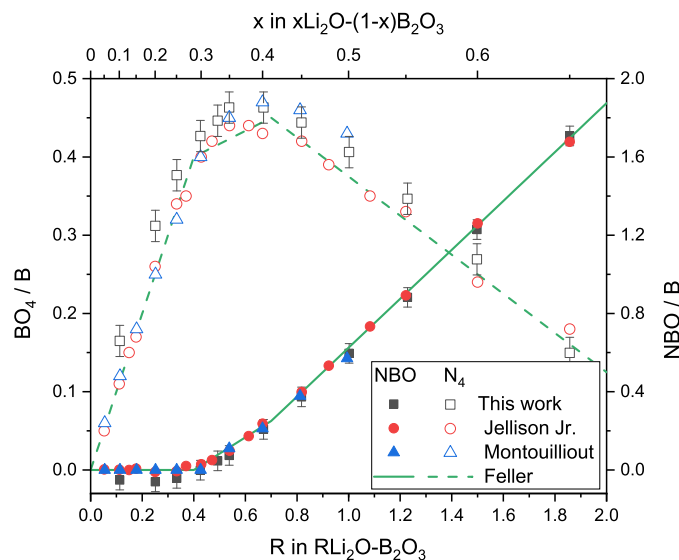**Fig. 1.** Fraction of non-bridging oxygens (NBO) and four coordinated borons (BO₄) per B calculated using Feller's model [12], and obtained experimentally via NMR by Montouillout [23], Jellison Jr. [11] and in this work, as a function of composition for Li₂O-B₂O₃ glasses.

while the scarce experimental results indicate that the plateau in the conductivity data persists to higher lithium concentrations [28,33]. This implies that the ionic conductivity of this glass may not be exclusively connected to the concentration of a specific lithium ion site, but to some other factor to be determined.

Recent works published by Montouillout [23] and Fan [10] relate the number of non-bridging oxygens to the change observed in the ionic conductivity of the glasses and melts. According to these works, the significant change observed at $R \approx 0.5$ is due to the boron anomaly, first observed by Biscoe and Warren in 1938 [4]. More specifically, the formation of the plateau in ionic conductivity is caused by the creation of non-bridging oxygens and eventual percolation of these sites. This relationship works well up to $R = 1.0$. This model does not explore the second change in behavior predicted by Takeda and collaborators [27].

To test the existence of this plateau, glasses with compositions up to $R = 1.85$ ($x = 0.65$) were prepared with the help of a fast roller quenching technique. This technique has been proved to be able to produce normally hard to obtain glasses [14]. The homogeneity of these glasses and their structure was tested to confirm that any behavior observed was strictly due to the glass and not a second phase.

2. Experimental procedure

Glasses were prepared by using well-mixed Li₂CO₃ and H₃BO₃ with over 99.5% purity obtained from the Sigma Aldrich Company. After 15 min of melting at 1000 °C in a platinum crucible, drops of melt were plate-quenched for values of $R = 0.1–1.0$, and roller-quenched at all higher concentrations. To account for possible errors in compositions, samples were weighed after the initial heating and found to be in good agreement with the predicted loss. All glasses were crushed into a fine powder with a mortar and pestle. The sample's properties were studied using differential scanning calorimetry, X-ray diffraction, Raman spectroscopy, and nuclear magnetic resonance.

It is known that many properties of glasses depend on their thermal history, including ionic conductivity [5]. The most common way to report the thermal history of a glass is by measuring its glass transition temperature (T_g). In this study, the T_g was obtained using a Perkin-Elmer Diamond differential scanning calorimeter (DSC). DSC was run from room temperature to 600 °C at a pace of 40 K/min. Experimental error was ±5 K determined by calibrating indium and zinc. To obtain the glass transition temperature the regression lines method was used [30].

X-ray diffraction (XRD) measurements of powdered glasses verified

the amorphous state of these materials. A Bruker D8 Discover XRD was operated on 0.30–0.50 g of each glass powder between 10 and 70° in 0.50° steps with 96 s timesteps at room temperature. The cathode ray current was 40 mA and 40 kV x-rays were obtained.

Raman spectra were recorded at the backscattering geometry on a Renishaw inVia Raman Microscope, equipped with a 2400 lines/mm diffraction grating, a high-sensitivity Peltier-cooled charge coupled device (CCD), a motorized xyz microscope stage, an x50 magnification lens and a Rayleigh rejection notch filter at 514.5 nm, allowing measurements down to 5 cm^{-1}. All measurements were performed at room temperature with a 2 cm^{-1} resolution, using the 514.5 nm line of an Ar ion laser for excitation. Each spectrum represents the average of 25 scans in the range 5–4000 cm^{-1} accumulated over 1.5 h, to improve the signal-to-noise ratio because of the powder form of glasses available for Raman measurements.

^{11}B nuclear magnetic resonance (NMR) was performed at 14.1 T on each sample to ensure phase purity and measure BO₃/BO₄ quantities. Powdered samples were packed into zirconia MAS rotors with Kel-F caps in a nitrogen glovebox. The rotors were spun at 10 kHz using room-temperature purified compressed air. The probe was tuned to 192.57 MHz and referenced to NaBH₄ at −42.06 ppm. A 45° tip angle was used (6 μs). The spectra were baseline corrected and the boron nitride probe background subtracted. The N₄ fraction was obtained by integrating BO₃ and BO₄ central transitions and first spinning sidebands. Saturation-recovery experiments were performed on all samples to measure the T_1 values. The ^{11}B T_1 relaxation time decreased with greater lithium content, consistent with an increase in mobility.

Electrical impedance spectroscopy (EIS) was conducted to examine the ionic conductivity of the glasses. For electrical measurements, powdered samples were poured into 0.635 cm diameter aluminum foil lined stainless steel molds and compressed mechanically into pellets. The powder was moistened with two drops of acetone and held at 1.4 kg/m^2 for 15 min with thickness varying between 1.0 and 1.9 mm. Once the metallic surfaces adhered to the glass, each sample's electrical response was obtained from a Gamry Instruments Interface 1010E Potentiostat/Galvanostat/ZRA impedance spectrometer. The impedance spectrometer applied excitation signals with 1500 mV across a frequency range of 1·10^5 to 1 Hz at working temperatures between 250 and 400 °C at 25 °C intervals.

From the values obtained for the real and imaginary part of the impedance as a function of the frequency, an equivalent RC circuit was found using Gamry's software (Gamry Framework) and assuming a
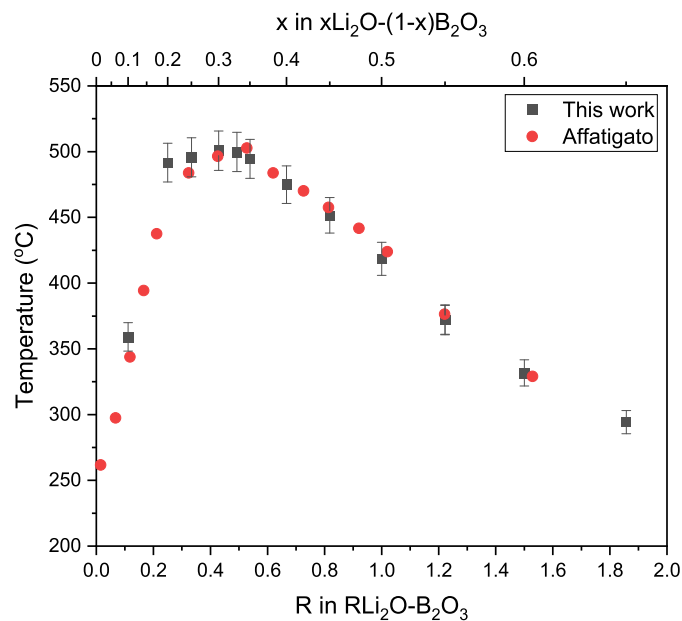
Fig. 2. Glass transition temperature (T_g) obtained via DSC in this work and from the literature [1].
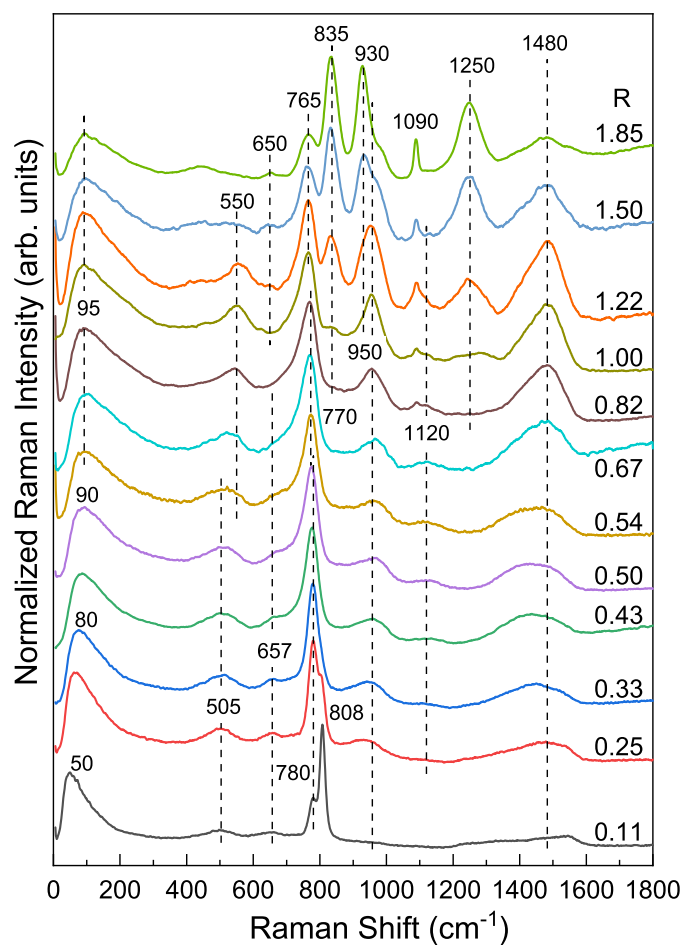

Fig. 3. Raman spectra for glasses $RLi_2O\text{-}B_2O_3$ in the range $0.11 \leq R \leq 1.85$. From left to right, the peaks correspond to the boson band (50–95 cm^{-1}), superstructural units containing boron tetrahedra (550, 765–780, 950, 1120 cm^{-1}), boroxol rings (808 cm^{-1}), pyroborate units (835, 1250 cm^{-1}), orthoborate units (930 cm^{-1}), CO_3^{2-} (1090 cm^{-1}) and metaborate triangles (1480 cm^{-1}) [7,15,21].

homogeneous material. The ionic conductivity (σ given in S·cm^{-1}) was then obtained using the equation:

$$\sigma = \frac{l}{A} \cdot \frac{1}{R_{DC}} \qquad (3)$$

where l and A are the sample's thickness (in cm) and area (in cm^2), respectively, and R_{DC} is the direct current resistance (in Ω), i.e. the resistance found with the equivalent circuit [3].

3. Results and discussion

3.1. Structural analysis

According to Feller et al. [12] and Jellison, Jr. et al. [11] the concentration of four-coordinated boron species (N_4) and of non-bridging oxygen (NBO) may be estimated as a function of R. There are three regions of interest; up to $R = 0.4$, all oxygen added to the system by the addition of Li$_2$O goes into the glass-forming network, increasing the number of N_4 without creating any NBOs. Between R = 0.4 and 0.7, NBOs are formed linearly as for each Li$_2$O added we create two non-bridging oxygens within the glass and the rate at which N_4 is created is reduced. Between $R = 0.7$ and 2 the N_4 fraction starts reducing as lithium oxide goes towards forming an increasing amount of non-bridging oxygen. From electroneutrality, it can be assumed that each four-coordinated borate unit has a Li$^+$ associated with it, denoted as Li^{Loose}. Similarly, each NBO has a Li$^+$ associated with it, denoted Li^{NB}. This model is seen in Fig. 1, which shows the fraction of N_4 and NBO per B obtained in this work, noting that $N_4 = BO_4/B$. In addition, experimental N_4 data were obtained by NMR from the literature [11,23], and this work.

The change in the structure of the glass affects many of its properties, including the glass transition temperature (T_g) [1] and many mechanical properties [13]. Values of T_g from this work and the literature are found in Fig. 2. Avramov [2] relates the solid electrolyte behavior as a function of the structure and network rigidity. In turn, the network rigidity is related mainly to the coordination number of the glass formers.

Raman results and peak attributions from the literature [7,15,21] corroborate the glass structure as given above. The spectra for $0.1 \leq R \leq 1.85$ are reported in Fig. 3. The most prominent development in the spectra is the decrease of the peak at ~808 cm^{-1} and the increase of a peak at ~780 cm^{-1} up to $R \leq 0.25$. According to the literature, this implies that the addition of alkali oxide to the glass transforms the boroxol rings (rings with three neutral BO$_3$ units) into rings with one BO$_4$ and two neutral BO$_3$ units. In the region $0.4 \leq R \leq 1.0$ the main Raman band shifts to ~770 cm^{-1} indicating the formation of borate rings with two BO$_4$ and one neutral BO$_3$ unit. Also, there is the appearance of weaker peaks at ~550 and 950 cm^{-1}, related to the development of superstructural groups like the diborate groups. Increasing R in the same composition range leads to increasing intensity at about 1480 cm^{-1}; this band manifests the formation of metaborate triangles having two bridging oxygens and one NBO, BO$_{2/2}$O$^-$. The appearance of the weak peak at ~835 cm^{-1} for $R = 1.0$ signals the formation of a new type of charged borate triangle i.e. the pyroborate unit (B$_2$O$_5^{4-}$) with 2 NBOs per boron. The relative population of B$_2$O$_5^{4-}$ units increases for $R \geq 0.5$ as shown by the fast development of the peaks at ~835 and ~1250 cm^{-1} characteristic of pyroborate units. At very high concentrations, the spectrum also shows the evolution of a peak at ~930 cm^{-1}, attributed to planar orthoborate units with 3 NBOs per boron, BO$_3^{3-}$. The peak at ~1090 cm^{-1} for $R \geq 1.0$ is associated to the presence of CO$_3^{2-}$ groups in the glass.

The progressive formation of triangular metaborate, pyroborate and orthoborate units shown by Raman spectroscopy for $R \geq 0.4$ results in an increase in the number of NBOs per boron, as found also by NMR spectroscopy on the same glasses (Fig. 1). As an example consider the Raman spectrum of the glass $R = 1.85$; it shows the presence of a small
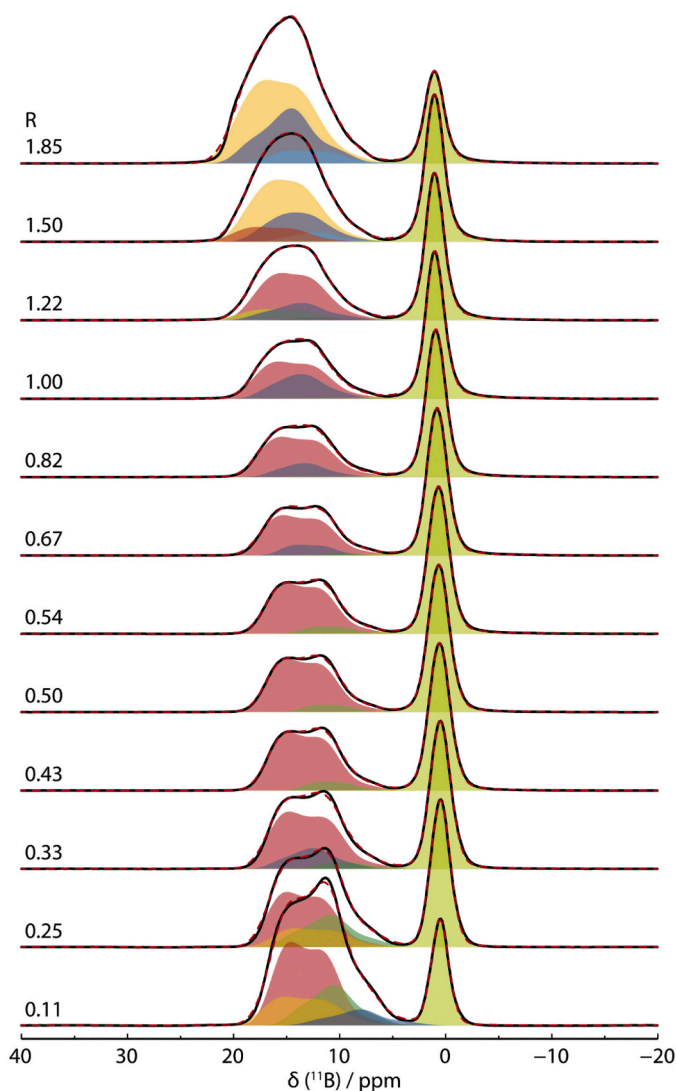

Fig. 4. ^{11}B MAS NMR spectra at 14.1 T for glasses RLi$_2$O-B$_2$O$_3$ in the range $0.11 \leq x \leq 1.85$. Each spectrum was deconvolved with the number of peaks determined by Monte Carlo error estimation. Peak shading is a guide for the eye and does not strictly correspond to common superstructural units.

concentration of rings with two BO$_4$ units and one neutral BO$_3$ unit (peak at ~765 cm^{-1}), relatively large amounts of B$_2$O$_5^{4-}$ (peaks at 835 and 1250 cm^{-1}), and BO$_3^{3-}$ units (peak at 930 cm^{-1}) and a small content of BO$_{2/2}$O$^-$ triangles (peak at ~1480 cm^{-1}). The Raman cross sections of the various units are not known at present to allow quantification of the borate speciation. In any case, the presence of these borate units at $R = 1.85$ leads eventually to $N_4 = 0.15$ and to NBO/B = 1.73 according to the present NMR results (Fig. 1).

A deconvolution of each ^{11}B MAS NMR spectrum for all twelve glasses is shown in Fig. 4. For each composition the BO$_3$ peaks (between 25 ppm and 5 ppm) show a variety of superstructural units, in agreement with the Raman spectra. The different species seen are mainly differentiated by ring, or non-ring BO$_3$, within a superstructural unit. As each composition contains its own particular mix of superstructural units, we expect a variety of lithium motion behaviors, per composition. This variety of motions combined with the changing composition makes modeling the lithium conductivity challenging and complex.

3.2. Electrical properties

The Nyquist diagrams and conductivity spectra resulted from the EIS
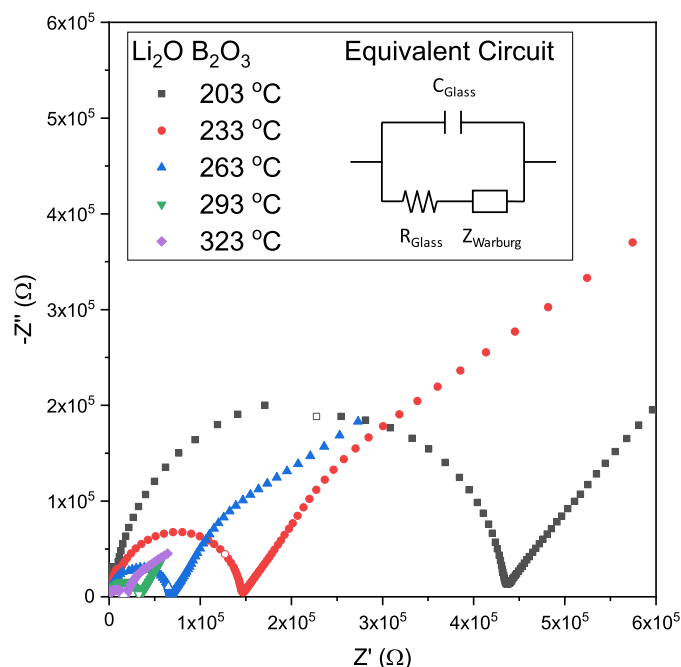
Fig. 5. Nyquist plot for the glass Li_2O-B_2O_3 ($R = 1$) at different temperatures. The sample behavior is typical for an ionic conductor with a single phase, also known as a Randles-Circuit (the system resistance is considered very small compared to the sample's resistance) [3]. The empty points correspond to a frequency of 10 kHz.
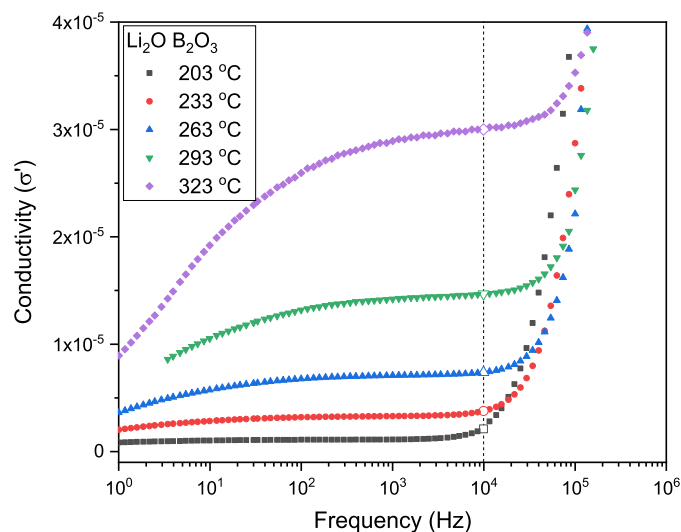
Fig. 6. Conductivity (in S/cm) spectra for the glass Li_2O-B_2O_3 ($R = 1$) at different temperatures. The sample behavior is typical for an ionic conductor with a single phase. The empty points correspond to a frequency of 10 kHz.

show a typical result for ionic single-phase samples. As an example, Fig. 5 presents the Nyquist diagram and Fig. 6 the conductivity spectra for Li_2O-B_2O_3 ($R = 1$) at different temperatures. In Fig. 5 is also given an example of the equivalent circuit used to calculate the direct current resistance of the samples, known as a Randles-Circuit (the system resistance is considered very small compared to the sample's resistance) [3]. Although the measurements were made on powdered samples, the sample behaved similarly to a bulk sample, with no detectable additional effects.

Verhoef [32] used the concept of structural changes described earlier to explain the ionic conductivity behavior of the lithium borate system, introducing the concept of two types of lithium sites in the glass matrix, Li^{Loose} and Li^{NB}. As expected, the existence of two different types of sites results in a significant change in the electrical properties of these glasses,

as seen by Montouillout [23], Elliott [9], Levasseur [34] and Matsuo [19]. Activation energies (E_A in eV) for the ionic conductivity can be obtained using the following Arrhenius equation:

$$\sigma \cdot T = \sigma_0 \cdot exp\left(-\frac{E_A}{k_B \cdot T}\right) \tag{4}$$

where σ_0 is a constant (in S·K·cm^{-1}), k_B is Boltzmann's constant and T is the temperature (in K). Kamitsos [16] used the Rice and Roth model [25] to calculate the activation energy using only vibrational parameters, as given by:

$$E_A = \frac{1}{2} m \cdot l_0^2 \cdot \nu_0^2 \tag{5}$$

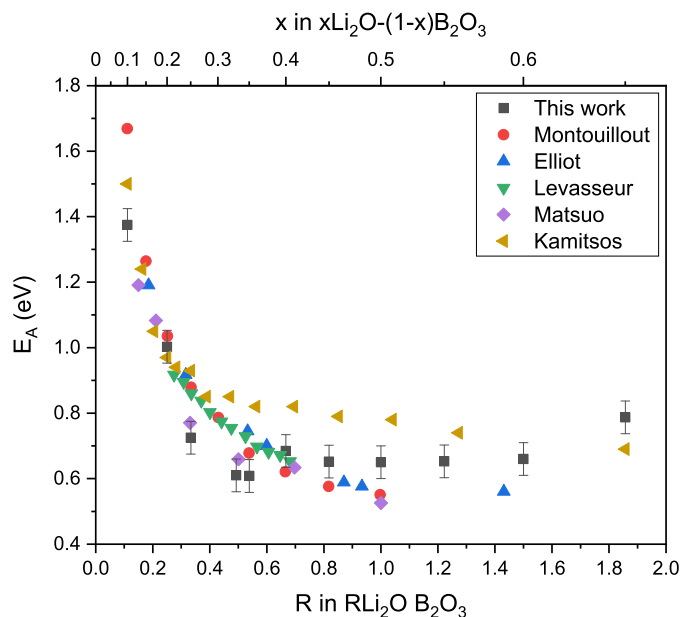where m is the mobile ion mass, l_0 is the hopping distance between

Fig. 7. Activation energy for the ionic conductivity as a function of composition for Li_2O-B_2O_3 glasses from this work and papers by Montouillout [23], Elliott [9], Levasseur [34], Matsuo [19] and Kamitsos [16].
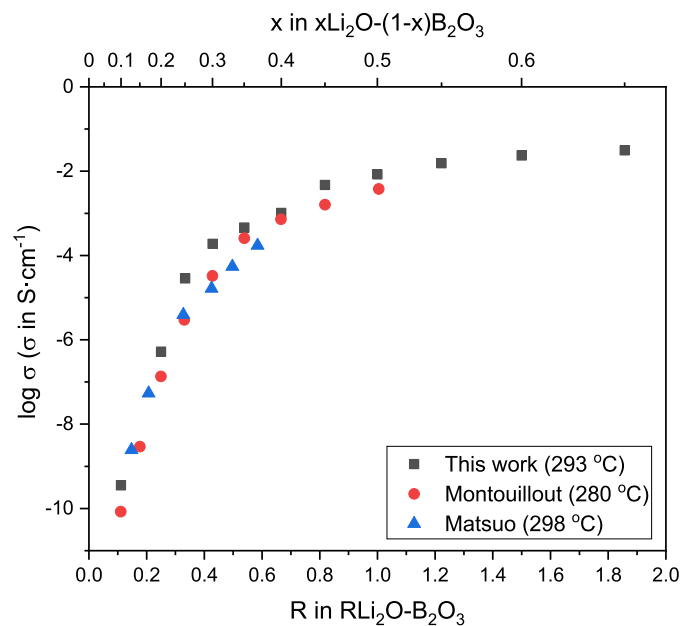

Fig. 8. Values of ionic conductivity at temperatures close to 290 °C as a function of composition for the glasses Li_2O-B_2O_3 for this work, Matsuo [19] and Montouillout [23]. Experimental errors are smaller than the point sizes.

neighboring sites and ν_0 is the cation-site vibrational frequency. Values found by this work follow the general trend observed in experimental results, although slightly higher than experimental results for higher Li^+ concentrations. It is important to notice that, although being able to distinguish between the two lithium sites in the far-infrared, the authors did not distinguish between them for the calculation of activation energies. Experimental values for the activation energy and predicted by using the Rice and Roth model are seen in Fig. 7.

The ionic conductivity of a glass may be given by the Nernst-Einstein equation [30]:

$$\sigma = \frac{n \cdot (Z \cdot e)^2 \cdot D}{k_b \cdot T} \qquad (6)$$

where n is the charge carrier density (given in cm^{-3}), Z is the valence of the charge carrier, e is the charge of an electron and D is the diffusion coefficient for the ionic conductivity process ($cm^2 \cdot s$). Values of ionic conductivity at temperatures close to 290 °C can be seen in Fig. 8.

One can assume that both n and D are activated processes, depending on temperature and composition, and the activation energy for the process relates to the activation energies of each of these two processes. Therefore, eq. (6) takes the form:

$$\sigma(T,R) \propto n(T,R) \cdot D(T,R) \qquad (7)$$

Looking at this problem exclusively through Eq. (7), two possible interpretations are commonly found in the literature to explain the
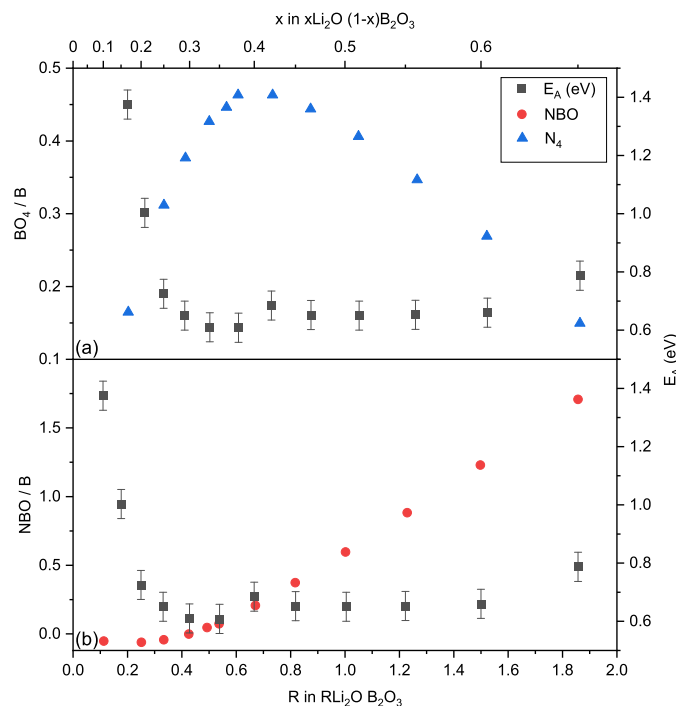
Fig. 9. BO$_4$ per B (a), NBOs per B (b) and activation energy (E$_A$ in eV) as a function of composition for the glasses studied in this work. The activation energy for the ionic conductivity of the glasses decreases with the addition of Li$_2$O following closely the formation of BO$_4$ species with fraction N$_4$, but reaches a limit when NBOs are formed within the glass ($R \geq 0.4$), even with the increase of the total concentration of Li$^+$.

changes in ionic conductivity within a glass system; either n is equal to the atomic density of the mobile ions in the glass and the conductivity is controlled by changes in D with temperature and composition, or the n is just a fraction of the mobile ions determined by a dissociation equilibrium and this dissociation equilibrium is what dictates the process. These two models are commonly referred to as the *strong electrolyte* model and the *weak electrolyte* model, respectively [18].

Values for activation energy of the ionic conductivity, N$_4$ and NBO fractions as a function of composition can be seen in Fig. 9. Experimental results of the electrical conductivity behavior of the studied glass system follows the total concentration of tetrahedral BO$_4$ units (N$_4$) and consequently the concentration of the Li$^+$ ions associated with them (Li^{Loose}) up to $R = 0.7$. When $R \leq 0.4$, the N$_4$ fraction increases and the activation energy for the ionic conductivity decreases, and when $0.4 \leq R \leq 0.7$ the total number of N$_4$ is increasing but with a slower rate. The newly added oxygen is assimilated into the glass structure as NBO and the Li$^+$ ions associated with them (Li^{NB}) do not appear to contribute significantly to the electrical properties of the glass. Therefore, the activation energy for the ionic conductivity seems to reach a plateau and does not change significantly with composition, implying that the diffusion coefficient of Li^{Loose} is significantly higher than Li^{NB}. This may be justified by the difference in the electrostatic strength of each pair.

Above R = 0.7, the N$_4$ decreases and the NBO formation rate increases, as seen in Figs. 1 and 9. If we follow the logic presented in the last paragraph, the ionic conductivity of the system should decrease proportionally to the decrease in the number of Li^{Loose}. On the other hand, using Takeda's topological model [27], the newly added Li$^+$, although being associated with NBO, are free to move and should add to the ionic conductivity of the system. Experimental results show that both values for activation energy as well as the absolute value of ionic conductivity stay relatively constant when $R > 0.7$. Therefore, the less diffusive species Li^{NB} must play a part in the ionic conductivity mechanism, even if it is not as efficient as the Li^{Loose}.

Considering that the ionic conductivity is given by Eq. (7), knowing that each of the two different species has its own diffusion coefficient (D) and its own density of charge carrier (n), defining the contribution of

each of the two species seems reasonable. First, one should consider that besides the existence of N$_4$ and NBO species, there are different types of NBO species and each of these species may have their own contribution to the ionic conductivity. Even so, it would still be possible to define the specific contribution of each species.

Unfortunately, a solution for this problem is far from trivial. To assume that all ions from a certain site are available to diffuse contradicts directly the weak electrolyte theory. According to the model, the addition of a few N$_4$ sites drastically increases the number of available ions for ionic conductivity, justifying the increase of the ionic conductivity by order of magnitudes with a linear increase in the N$_4$ concentration. Not only that, at high concentrations one has to consider the percolation effects, observed by Varsamis [29]. With a high concentration of Li$^+$, these ions may experience more than one type of site simultaneously, making it harder to separate the effect of the individual sites exclusively. A way to verify the possible existence of different mechanisms for the ionic conductivity could be resolved by the Funke and Roling universality scaling [26], but our results were inconclusive due the lower frequency range of our EIS system.

4. Conclusion

Lithium borate glasses with $R \leq 1.85$ were prepared with the help of rapid cooling. These glasses were used to test the relationship between the number of Li^{Loose} and the ionic conductivity of these glasses. The general behavior for ionic conductivity follows the concentration of BO$_4$ species (N$_4$) and consequently the Li^{Loose} concentration quite well up to $R = 0.7$. Above this value, there is a breakdown where the Li^{Loose} decreases but experimental values of ionic conductivity and activation energy remain constant.

Structural analysis paired with ionic conductivity results imply that it is not exclusively the number of Li^{Loose} ions that regulate the electrical properties of the glass, but also the number Li^{NB} associated with non-bridging oxygen (NBO) within the glass. As they form at concentrations of $R \geq 0.4$, the Li$^+$ ions associated with NBOs have a less efficient contribution to the ionic conductivity, that could be justified by the

difference in the electrostatic strength of each pair, but the ionic conductivity follows a plateau even with the increase of the number of NBOs and the decrease of the available BO$_4$ sites.

Declaration of Competing Interest

The authors declare that they have no known competing financial interests or personal relationships that could have appeared to influence the work reported in this paper.

Acknowledgments

References

[1] M. Affatigato, S. Feller, E.J. Khaw, D. Feil, B. Teoh, O. Mathews, The glass transition temperature of lithium and lithium-sodium borate glasses over wide ranges of composition, Phys. Chem. Glasses 31 (1) (1990) 19–24.

[2] I. Avramov, Rigid-floppy percolation threshold, J. Phys. Condens. Matter 21 (21) (2009).

[3] E. Barsoukov, J.R. Macdonald, Impedance Spectroscopy, Wiley, 2005.

[4] J. Biscoe, B.E. Warren, X-ray diffraction study of soda-boric oxide glass, J. Am. Ceram. Soc. 21 (8) (1938) 287–293.

[5] C.B. Bragatto, D.R. Cassar, O. Peitl, J.-L. Souquet, A.C.M. Rodrigues, Structural relaxation in AgPO$_3$ glass followed by in situ ionic conductivity measurements, J. Non-Cryst. Solids 437 (2016) 43–47.

[6] B.V.R. Chowdari, R. Zhou, The role of Bi$_2$O$_3$ as a network modifier and a network former in x Bi$_2$I$_3$·(1-x) LiBO$_2$ glass system, Solid State Ionics 90 (1996) 151–160.

[7] G.D. Chryssikos, E.I. Kamitsos, M.A. Karakassides, Structure of borate glasses. Part 2. Alkali induced network modifications in terms of structure and properties, Phys. Chem. Glasses 31 (3) (1990) 109–116.

[8] J.C. Dyre, P. Maass, B. Roling, D.L. Sidebottom, Fundamental questions relating to ion conduction in disordered solids, Rep. Prog. Phys. 72 (2009), 046501.

[9] R.J. Elliott, L. Perondi, R.A. Barrio, Ionic conduction in (1-x)B$_2$O$_3$ + xLi$_2$O, J. Non-Cryst. Solids 168 (1–2) (1994) 167–178.

[10] H. Fan, L. del Campo, V. Valérie Montouillout, M. Malk, Ionic conductivity and boron anomaly in binary lithium borate melts, J. Non-Cryst. Solids 543 (2020) 120160/1–8.

[11] G.E. Jellison Jr., S.A. Feller, P.J. Bray, A re-examination of the fraction of 4-coordinated boron atoms in the lithium borate glass system, Phys. Chem. Glasses 19 (1978) 52–53.

[12] S.A. Feller, W.J. Dell, P.J. Bray, ^{10}B NMR studies of lithium borate glasses, J. Non-Cryst. Solids 51 (1) (1982) 21–30.

[13] Y. Fukawa, Y. Matsuda, Y. Ike, M. Kodama, S. Kojima, Glass transitions and elastic properties of lithium borate glasses over a wide composition range studied by micro-brillouin scattering, Jpn. J. Appl. Phys. 47 (5 Part 2) (2008) 3833–3835.

[14] A.J. Havel, S.A. Feller, M. Affatigato, M. Karns, Design and operation of a new roller quencher for rapidly cooling melts into glasses, Glass Technol. Eur. J. Glass Sci. Technol. Part A 50 (4) (2009) 227–229.

[15] E.I. Kamitsos, G.D. Chryssikos, Borate glass structure by Raman and infrared spectroscopies, J. Mol. Struct. 247 (C) (1991) 1–16.

[16] E.I. Kamitsos, A.P. Patsis, M.A. Karakassides, G.D. Chryssikos, Far infrared spectra of binary alkali borate glasses, Solid State Ionics 28-30 (1988) 687–692.

[17] E.I. Kamitsos, A.P. Patsis, M.A. Karakassides, G.D. Chryssikos, Infrared reflectance spectra of lithium borate glasses, J. Non-Cryst. Solids 126 (1990) 52–67.

[18] S.W. Martin, C.A. Angell, DC and AC conductivity in wide composition range Li2OP2O5 glasses, J. Non-Cryst. Solids 83 (1–2) (1986) 185–207.

[19] T. Matsuo, M. Shibasaki, T. Katsumata, Diffusion of Li ion in glassy Li$_2$O·B$_2$O$_3$ system, Solid State Ionics 154–155 (2002) 759–766.

[21] B.N. Meera, J. Ramakrishna, Raman spectral studies of borate glasses, J. Non-Cryst. Solids 159 (1993) 1–2, 1–21.

[22] T. Minami, in: Tsutomu Minami, M. Tatsumisago, M. Wakihara, C. Iwakura, S. Kohjiya, I. Tanaka (Eds.), Solid State Ionics for Batteries, Springer-Verlag, Tokyo, 2005.

[23] V. Montouillout, H. Fan, L. del Campo, S. Ory, A. Rakhmatullin, F. Fayon, M. Malki, Ionic conductivity of lithium borate glasses and local structure probed by high resolution solid-state NMR, J. Non-Cryst. Solids 484 (November 2017) (2018) 57–64.

[24] A. Pradel, M. Ribes, Ionic conductive glasses, Mater. Sci. Eng. B 3 (1989) 45–56.

[25] M.J. Rice, W.L. Roth, Ionic transport in super ionic conductors: a theoretical model, J. Solid State Chem. 4 (1971) 294–310.

[26] B. Roling, A. Happe, K. Funke, M.D. Ingram, Carrier concentrations and relaxation spectroscopy: new information from scaling properties of conductivity spectra in ionically conducting glasses, Phys. Rev. Lett. 78 (1997) 2160.

[27] W. Takeda, C.J. Wilkinson, S.A. Feller, J.C. Mauro, Topological constraint model of high lithium content borate glasses, J. Non-Cryst. Solids X3 (2019) 100028/1–5.

[28] M. Tatsumisago, T. Minami, Lithium ion conducting glasses prepared by rapid quenching, Mater. Chem. Phys. 18 (1–2) (1987) 1–17.

[29] C.P.E. Varsamis, A. Vegiri, E.I. Kamitsos, Molecular dynamics investigation of lithium borate glasses: local structure and ion dynamics, Phys. Rev. B 65 (10) (2002) 1–14.

[30] A.K. Varshneya, Fundamentals of Inorganic Glasses, Academic Press, 1994.

[31] A. Vegiri, C.P.E. Varsamis, Clustering and percolation in lithium borate glasses, J. Chem. Phys. 120 (16) (2004) 7689–7695.

[32] A.H. Verhoef, H.W. den Hartog, High-frequency dielectric properties of alkali and alkali-halide borate glasses, Solid State Ionics 68 (3–4) (1994) 305–315.

[33] M. Yamashita, R. Terai, Ionic conductivity of Li$_2$O-B$_2$O$_3$-Li$_2$SO$_4$ glasses, Glas. Berichte-Glas. Sci. Technol. 63 (1990) 13–17.

[34] A. Levasseur, M. Menetrier, Borate based lithium conducting glasses, Materials Chemistry and Physics 23 (1–2) (1989) 1–12, https://doi.org/10.1016/0254-0584(89)90013-8, 34.